Atom and Ion Chemistry in Low Pressure Hydrogen DC Plasmas

I. Méndez,[†] F. J. Gordillo-Vázquez,[‡] V. J. Herrero,*,[†] and I. Tanarro*,[†]

Instituto de Estructura de la Materia, CSIC, Serrano 123, 28006 Madrid, Spain, and Instituto de Óptica, CSIC, Serrano 121, 28006 Madrid, Spain

The chemical composition of a low-pressure hydrogen dc plasma produced in a hollow cathode discharge has been measured and modeled. The concentrations of H atoms and of H^+, H_2^+ and H_3^+ ions were determined with a combination of optical spectroscopic and mass spectrometric techniques, over the range of pressures ($p \sim 0.008-0.2$ mbar) investigated. The results were rationalized with the help of a zero-order kinetic model. A comparatively high fraction ($\sim 0.1 \pm 0.05$) of H atoms, indicative of a relatively small wall recombination, was observed. Low ionization degrees ($<10^{-4}$) were obtained in all cases. In general, the ionic composition of the plasma was found to be dominated by H_3^+, except at the lowest pressures, where H_2^+ was the major ion. The key physicochemical processes determining the plasma composition were identified from the comparison of experimental and model results, and are discussed in the paper.

Introduction

Low-pressure plasmas of hydrogen and hydrogen mixtures play a key role in a variety of environments including planetary ionospheres and interstellar media, controlled fusion devices, and technological processes. Hydrogen atoms, atomic and molecular ions, and excited molecules determine the chemistry and energy transfer in all these plasmas, but the relative importance of the different physicochemical processes, and thus the concentrations of the various unstable species, depend on the particular plasma conditions. The primary H_2^+ and H^+ ions, formed in the direct or dissociative ionization of the molecular precursor, are usually accompanied by H_3^+, which is often dominant. This ionic species is basic for the generation of a large number of the molecules observed in the interstellar space.[1,2] Since its landmark IR laboratory detection by T. Oka in the 1980s,[3] its ubiquity has been established in numerous observations (see ref 4 and references therein). Many studies have also been devoted to the atomic hydrogen produced in these plasmas, which is of relevance for film deposition processes.[5−8] The dynamics of internally excited states of H_2[9−18] and its close relationship to the production of H^- ions by dissociative electron attachment have been also addressed by various groups.[19−21]

Theoretical and experimental investigations over decades have provided much information on fundamental processes relevant to H_2 plasmas (see for instance refs 22−27 and references therein), but there is still a dearth of basic data specially on state-resolved cross sections and on gas surface interactions, and many uncertainties remain about the coupling between the plasma chemistry and the discharge dynamics. In general, combined theoretical and experimental studies are needed in order to validate many of the data and to identify key processes in particular H_2 plasmas. Most work thus far has centered on moderate pressure (>0.5 mbar) MW or RF discharges, which

are the usual choice for plasma-enhanced chemical vapor deposition (PECVD) reactors (see refs 6, 18, 28−30 and the references cited in these works). For lower pressures and other types of discharge, studies have not been so frequent.

In a recent work, Hollmann and Pigarov[31] have reported measurements of molecular ion concentrations in a hydrogen reflex-arc discharge. The experimental setup was designed for the simulation of plasmas occurring at the divertor of fusion devices.[32,33] A plasma, generated with high electron densities and temperatures in the arc region, and consisting mostly of H^+ ions, enters a neighboring chamber where it hits a target gas (in this case also hydrogen). The plasma in the target chamber corresponds to gas pressures of $0.2-4 \times 10^{-2}$ mbar, electron densities of $10^{11}-10^{12}$ cm^{-3} and electron temperatures of $3-7$ eV. Very high vibrational temperatures of H_2 were obtained in all cases. The relative ion concentrations were seen to vary drastically within the experimental range. For the conditions of the experiments, the measured ion concentrations could be approximately modeled using a reduced set of rate equations and cross-section data from the literature.

In this work, we have explored a different regime. We present a detailed diagnostics and modeling of low pressure hydrogen plasmas generated in a hollow cathode reactor. The power density is appreciably smaller than that usual in MW and RF discharges. Gas pressures and electron temperatures are similar to those of the just mentioned work of Hollmann and Pigarov,[31] but the mechanism of initiation of the discharge is different and the electron densities are much lower. The key physicochemical processes determining the chemical composition of the plasma are identified and discussed.

Experimental Section

The experimental plasma reactor, shown in Figure 1, is basically the same as in our previous works on air plasmas[34] and $H_2 + CH_4 + N_2$ plasmas.[35,36] It consists of a grounded cylindrical stainless steel vessel (10 cm diameter, 34 cm length) and a central anode. The vessel walls are provided with a number of ports for connection of gas inlets, diagnostics tools, observation windows, and pressure gauges.

* Corresponding authors. Fax: +34.91.5645557. E-mail: (I.T.) itanarro@iem.cfmac.csic.es; (V.J.H.) vherrero@iem.cfmac.csic.es.
† Instituto de Estructura de la Materia, CSIC.
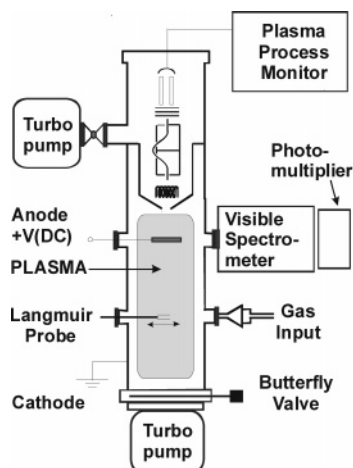‡ Instituto de Óptica, CSIC, Serrano 121, 28006 Madrid, Spain.

Low Pressure Hydrogen DC Plasmas

J. Phys. Chem. A, Vol. 110, No. 18, 2006 **6061**

Figure 1. Experimental setup.

The reactor was continuously pumped by a 450 L/s turbomolecular pump to a base pressure of 10^{-6} mbar. The desired reactor pressure was selected by balancing the input H_2 flow with a needle valve in the gas inlet, and the output flow, with a butterfly valve throttled at the exit of the reactor. In general, the position of the butterfly valve was kept fixed during the experiments, and the chamber pressure was controlled with the needle valve at the entrance. Gas pressures in the 0.008–0.2 mbar range, as measured with a capacitance manometer, were used for plasma generation. Residence times of the gas in the reactor were always found to be 1 ± 0.1 s, independent of the gas pressure. They were determined by quickly closing a shutoff valve at the entrance and measuring the time evolution of the 2 amu peak in the plasma monitor (see below). These residence times are much longer than the characteristic times of all relevant kinetic processes. The reactor was electrically fed by a 0.2 A, 2000V, dc source through a 100 Ω ballast resistor. At the lowest operating pressures, an electron gun built in the laboratory[34] was used for ignition of the plasma. Steady-state plasma currents, $I_p \approx 150$ mA in the abnormal glow discharge mode, with output source voltages ~400–460 V, were maintained during the experiments. Under these conditions, the wall reactor reached a temperature of 48 ± 4 °C, as measured with a thermocouple.

The radial distribution of electron density, N_e, and electron mean temperature, T_e, in the plasma volume were measured with a double Langmuir probe designed in our laboratory.[37] Although double Langmuir probes are only sensitive to ion densities in the saturation regions of their characteristic curve, charge neutrality of the plasma has been assumed in the negative glow to deduce N_e.

For the evaluation of the data, the approximation of orbital limited motion in a collision free probe sheath for electropositive plasma was used.[38–40] This approximation holds when the mean free path, λ, is much larger than the Debye length, λ_D, and λ_D is comparable to the probe radius, r_p. In the present experiments, $\lambda \approx 2{-}0.5$ cm, $\lambda_D \approx 200{-}74$ μm and $r_p = 65$ μm. The average ion mass was used in each case for the derivation of charge densities. Note that the estimate of T_e from double Langmuir probe measurements implies the assumption of a Maxwellian electron energy distribution function.

A Plasma Process Monitor, Balzers PPM421, was used for the detection of both neutrals and ions from the plasma. It consists of an electron bombardment ionizer, an electrostatic focusing system, a cylindrical mirror energy analyzer, and a quadrupole mass filter, with a secondary electron multiplier in the counting mode. For the detection of ions, the electron bombardment ionizer was switched off and the ions were allowed to enter the detector directly from the plasma. The apparatus was installed in a differentially pumped chamber connected to the reactor through a 100 μm diaphragm. During operation, the pressure in the detection chamber was kept in the 10^{-7} mbar range by means of a turbomolecular pump. The ion flux ratio for each m/q^+ ratio was obtained by integrating its individual ion energy distributions. Absolute concentrations of ions were obtained by scaling the total sum of the relative ion densities to the measured mean charge density. The relative sensitivity of the plasma monitor (including electrical filters and electron multiplier) for masses lower than 4 was checked by filling the chamber of the PPM421 with a small pressure of H_2 or He and comparing the PPM signal with the reading of a Bayard-Alpert gauge. For mass 1, the spectra of H_2, CH_4 and H_2O were compared with known fragmentation patterns for these substances.[41] To calibrate the relative sensitivity of the secondary electron multiplier to the H_3^+ ions, the intensity ratio between H_3^+ and H_2^+ was measured in a discharge of H_2 and compared with that of a Faraday cup available as secondary detector in the plasma monitor.

Internal temperatures of the H_2 molecules and H atom concentrations were derived from optical emission spectroscopy (OES) measurements carried out with an assembly of a 1/4 m monochromator (Oriel 77200 with a grating of 1200 grooves /mm and slits of 120 or 10 μm) and a photomultiplier (Hamamatsu R928). The spectral response of the spectrometer was checked with a calibrated tungsten lamp.

The vibrational temperatures, T_v, of the H_2 molecules were obtained from emission lines of the Fulcher-α band of H_2, starting from molecules excited to the $d^3\Pi_u$ state by electron impact. In particular Q1 branch ($\Delta J = 0$) lines corresponding to $a^3\Sigma_g^+$, v, $J = 1 \leftarrow d^3\Pi_u$, v, $J = 1$ transitions were selected for the temperature estimate. The collisional radiative model of Lavrov et al.[42] was used to correlate the T_v in the ground ($X^1\Sigma_g^+$) electronic state of H_2 with the measured emission lines. Franck–Condon factors for electron impact $X^1\Sigma_g^+$, $v \to d^3\Pi_u$, v' excitation, radiative lifetimes of the $d^3\Pi_u$, v, $J = 1$ levels, and spontaneous emission transition probabilities were taken from ref 42. Estimates of T_v using the J-integrated density of each vibrational level led to the same results.

The rotational temperatures of H_2 molecules in the ground electronic state were also estimated from emission lines of the Fulcher-α system as indicated in ref 43. Boltzmann rotational distributions at the gas temperature were inferred from this analysis (see below) indicating an effective equilibrium between translation and rotation in the plasmas.

The ratio of the concentrations of atomic and molecular hydrogen, $[H]/[H_2]$, was determined from the quotient between the intensity of the emission lines $I_H\alpha$ (656.5 nm) and $I_H\beta$ (486.1 nm) of the Balmer series of atomic hydrogen, following the procedure indicated by Lavrov et al. (see eq 10 of ref 44). Besides the measured line intensities, the method requires the knowledge of T_e, determined with the Langmuir probe as indicated above, and the emission rate coefficients of the Balmer-α,β lines for direct and dissociative electron impact excitation processes, which were taken from refs 45 and 46. Emissions from dissociative recombination of H_2^+ and H_3^+ have been neglected in the evaluation of H concentration from spectroscopic data because the concentrations of these ions are much lower than those of H_2 and H. An independent estimate of the [H] concentration was obtained from actinometric measurements, for discharge pressures where T_e was not too

TABLE 1: Homogeneous Reactions Considered[a]

reactions	rate coeff expression (cm^3 s^{-1})
1. $H + e \rightarrow H^+ + 2e$	$k_1 = 6.5023 \times 10^{-9} \times T_e^{0.48931} \times e^{-12.89365/T_e}$
2. $H_2 + e \rightarrow H^+ + H + 2e$	$k_2 = 2.9962 \times 10^{-8} \times T_e^{0.44456} \times e^{-37.72836/T_e}$
3. $H_2^+ + e \rightarrow H^+ + H + e$	$k_3 = 1.0702 \times 10^{-7} \times T_e^{0.04876} \times e^{-9.69028/T_e}$
4. $H_2^+ + e \rightarrow H^+ + H^+ + 2e$	$k_4 = 2.1202 \times 10^{-9} \times T_e^{0.31394} \times e^{-23.29885/T_e}$
5. $H_2^+ + H \rightarrow H_2 + H^+$	$k_5 = 9.0 \times 10^{-10}$
6. $H_2 + H^+ \rightarrow H_2^+ + H$	$k_6 = 1.19 \times 10^{-22}$
7. $H_2 + e \rightarrow H_2^+ + 2e$	$k_7 = 3.1228 \times 10^{-8} \times T_e^{0.17156} \times e^{-20.07734/T_e}$
8. $H_3^+ + e \rightarrow H_2^+ + H + e$	$k_8 = 4.8462 \times 10^{-7} \times T_e^{-0.04975} \times e^{-19.16565/T_e}$
9. $H_2^+ + e \rightarrow H^* + H$	$k_9{}^b = a + b \times T_e + c \times T_e^2 + d \times T_e^3 + e \times T_e^4$
10. $H_2^+ + H_2 \rightarrow H_3^+ + H$	$k_{10} = 2.60 \times 10^{-9}$
11. $H_3^+ + e \rightarrow 3 H$	$k_{11} = 0.5 \times K^c$
12. $H_3^+ + e \rightarrow H_2 + H$	$k_{12} = 0.5 \times K^c$
13. $H_2 + e \rightarrow 2 H + e$	$k_{13} = 1.7527 \times 10^{-7} \times T_e^{-1.23668} \times e^{-12.59243/T_e}$

[a] The values of T_e are in eV. [b] $a = 7.51371 \times 10^{-9}$, $b = -1.11516 \times 10^{-9}$, $c = 1.03156 \times 10^{-10}$, $d = -4.14905 \times 10^{-12}$, and $e = 5.85916 \times 10^{-14}$. [c] $K = 8.39247 \times 10^{-9} + 3.01631 \times 10^{-9} \times T_e - 3.80439 \times 10^{-10} \times T_e^2 + 1.31108 \times 10^{-11} \times T_e^3 + 2.41631 \times 10^{-13} \times T_e^4 - 2.29832 \times 10^{-14} \times T_e^5 + 3.5472 \times 10^{-16} \times T_e^6$.

TABLE 2: Heterogeneous Reactions Considered

reaction	rate coeff expression
1.- $H + wall \rightarrow H_2$	$\gamma = 0.03$ (see text)
2.- $H^+ + wall \rightarrow H$	$\gamma^+ = 0.9$
3.- $H_3^+ + wall \rightarrow H_2 + H$	$\gamma^+ = 0.9$

high, by comparing the intensity of the H_β transition with that of the $(2p^9 \rightarrow 1s^5)$ transition of Ar (811.5 nm) in H_2 plasmas containing 5% of Ar. Rate coefficients for electron impact excitation of Ar were obtained from the cross sections of ref 47. In previous publications,[6,7] the reliability of this procedure had been questioned, especially for high electron temperatures and low fractions of atomic hydrogen, due to the unfavorable competition between emission from direct and dissociative excitation. However, the new excitation rate constant data of Lavrov and Pipa[45,46] indicate that the range of applicability is larger than previously assumed. In addition, the comparatively large H fraction obtained in our experiments renders the method more suitable. As shown below, consistent values of the H concentration are obtained with the two different spectroscopic methods. This agreement strengthens the confidence in the measured values.

Kinetic Model

To model the nonequilibrium ion chemistry of our low-pressure dc hollow cathode H_2 plasma, we have developed a simple zero order kinetic model for solving the ion and atomic hydrogen rate equations. It is based on the numerical integration of a system of coupled differential equations accounting for the time evolution of the various plasma species from the ignition of the discharge to the steady state. The input parameters of our model are the pressure in the plasma reactor, the measured values of the electron temperature and electron density as a function of the pressure and that of the vibrational temperature of H_2. All these parameters have been experimentally determined (see next section). Additionally, T_e values were selected in the model, within the limits given by the experimental error bars, to get the best fit to the data. We have assumed that the value of the ion temperature (T_{ion}) is equal to that of the gas temperature ($T_{gas} = 300$ K). Our goal is to calculate the concentrations of atomic hydrogen and of the ions H^+, H_2^+, and H_3^+. The concentration of the latter species in the plasma is assumed to be controlled by the set of homogeneous and heterogeneous reactions shown in Tables 1 and 2, respectively. The (electron and ion) rate coefficients are the same as those used by Hollman and Pigarov.[27,31,48] For computational purposes, most of the electron-driven rate coefficients have been fitted

when possible to the convenient expression $k_i = a \times T_e^b \times \exp(c/T_e)$ cm^3 s^{-1}. The expressions for k_9, k_{11}, and k_{12} are more cumbersome than those for k_i ($i = 1, ..., 8$, and 13) but are also listed in Table 1. In all cases, the electron-impact rate coefficients have been calculated under the assumption that the free plasma electrons follow a Maxwellian electron energy distribution. To show the accuracy of the fitted expressions to the data taken from ref 31, we have plotted two representative rate coefficients like k_7 and k_{11} in the two panels of Figure 2. The lower panel of this figure shows the rate coefficients for the electron impact neutralization of H_3^+. In accordance with the results of ref 49, the two possible output channels ($H_2 + H$ and $H + H + H$) are assumed to have equal probability over the range of energies relevant to the present work. The particle H^* in Table 1 refers to electronically excited atomic hydrogen, which is assumed to deactivate radiatively.

The balance equations solved to describe the kinetics of atomic hydrogen and ion concentrations are

$$\frac{\partial N_2}{\partial t} = N_{H_2}(N_e k_7 + N_1 k_6) + N_3 N_e k_8 - N_2(N_e k_3 + N_e k_4 +$$
$$N_e k_9 + N_{H_2} k_{10} + N_H k_5) - \frac{N_2}{\tau_2} \quad (1)$$

$$\frac{\partial N_3}{\partial t} = N_2 N_{H_2} k_{10} - N_e N_3 (k_8 + k_{11} + k_{12}) - \frac{N_3}{\tau_3} \quad (2)$$

$$\frac{\partial N_H}{\partial t} = 2 N_e N_{H_2} k_{13} + 3 N_e N_3 k_{11} + N_e N_3 k_{12} + N_2 N_{H_2} k_{10} +$$
$$2 N_e N_2 k_9 + N_e N_3 k_8 + N_1 N_{H_2} k_6 + N_e N_2 k_3 + N_e N_2 k_2 -$$
$$N_e N_H k_1 - N_2 N_H k_5 + \gamma^+ \frac{N_1}{\tau_1} + \gamma^+ \frac{N_3}{\tau_3} - N_H \left(\frac{1}{\tau_{dif} + \tau_{wall}} \right) \quad (3)$$

and the plasma electrical charge neutrality equation

$$N_e = N_1 + N_2 + N_3 \quad (4)$$

where N_1, N_2, N_3, N_H and N_e stand for the concentrations of the atomic ions H^+, H_2^+, and H_3^+, hydrogen atoms, and electrons in the plasma, respectively. The magnitude γ^+ stands for the probability of H^+ and H_3^+ ions to recombine at the reactor walls producing H atoms. We have also assumed that the ions are lost to the reactor walls on different time scales τ_i characteristic of each ion, which is inversely proportional to the square root

Low Pressure Hydrogen DC Plasmas

J. Phys. Chem. A, Vol. 110, No. 18, 2006 **6063**
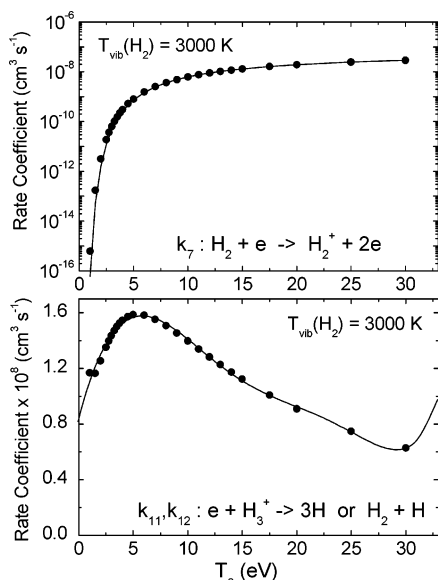
Figure 2. Rate coefficients for electron impact ionization of H_2, k_7 (upper panel), and for the electron impact neutralization of H_3^+, k_{11} (lower panel). Dots: data from ref 31, lines: fitted expressions to the data used in the present model (see Table 1). Note that the same rate coefficient has been used for the two output channels of reaction 11 (see text).
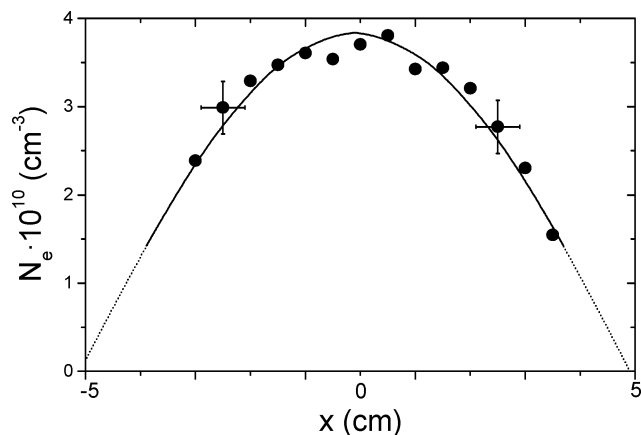

Figure 3. Dots: Experimental dependence of electron density, N_e, with radial position, x, in the cylindrical hollow cathode reactor, measured with the double Langmuir probe for a 0.2 mbar H_2 discharge; error bars indicate the uncertainties in the Langmuir probe results. Continuous line: cosine function normalized to the experimental maximum; this is the approximate behavior expected for the plasma in a cylindrical geometry.[51]

of its mass.[34] Thus, the ion lifetimes τ_i are given by the expressions

$$\tau_i^{-1} = \frac{N_H N_e k_1 + N_{H_2} N_e (k_2 + k_7)}{\sqrt{m_i} \sum_{j=1}^{3} \dfrac{N_j}{\sqrt{m_j}}} \quad (5)$$

where N_i and m_i are the ion concentration and ion mass, which runs from $m_1 = 1$ (H^+) to $m_3 = 3$ (H_3^+), respectively. The processes considered in the numerator of eq 5 are only those that contribute to the creation of a net electrical charge in the plasma. Therefore, mechanisms such as charge-transfer reactions are not taken into account. As can be noted in expression 3, the recombination of hydrogen atoms in the reactor walls and H atom diffusion have been considered as possible loss channels of atomic hydrogen. To evaluate τ_{dif} and τ_{wall}, we have considered the following expressions

$$\tau_{dif} = \frac{\Lambda^2}{D_H} \text{ and } \tau_{wall} = \frac{4V}{A} \frac{1}{\gamma \langle v_{th} \rangle} \quad (6)$$

where Λ is a characteristic diffusion length, D_H is the diffusion coefficient of atomic hydrogen, V and A are the volume and area of the reactor considered, γ is the H wall recombination probability to produce H_2, and $\langle v_{th} \rangle$ is the mean thermal speed of H at $T_{gas} = 300$ K, which is in fact a lower limit (the actual temperature of H atoms, produced initially with higher energies in the electron impact dissociation of H_2, is not known). As indicated below, even for this limiting case the recombination process is not determined by diffusion. The diffusion coefficient considered for H is $D_H = 1574/P$ (cm^2 s^{-1}), and is valid for H_2 environments at $T_{gas} = 300$ K. Since we are dealing with a cylindrical reactor with a radius $R = 5$ cm and a length $L = 34$ cm, the characteristic diffusion length[50] is $\Lambda = R/2.405$ cm = 4.32 cm. In solving the system of eqs 1–4, we have also assumed that both H^+ and H_3^+ hit the reactor walls and recycle

atomic hydrogen into the plasma with the same probability $\gamma^+ = 0.9$ (see Table 2).[31]

Results and Discussion

Figure 3 shows a typical radial profile of electron density for a 0.2 mbar discharge, measured with a probe placed at about 15 cm from the anode (see Figure 1). In fact the probe is sensitive to the total positive ion concentration, but we have assumed that, for our plasmas, negative ions (H^-) can be neglected and thus the plasma electroneutrality guarantees equal concentrations of ions and electrons. Under our conditions, this is a reasonable assumption since H^- ions, mainly formed in collisions of electrons with vibrationally excited H_2 molecules, are not expected to have appreciable concentrations for T_v values lower than 3000 K,[20,22] as found in the present experiments (see below and lower panel of Figure 4).

In the central part of the reactor, the electron density presents a nearly constant value of about 3.5×10^{10} cm^{-3} within a radius of $\approx 1.5-2$ cm around the axis. Note that the resolution of these measurements is limited by the 8 mm active length of the Langmuir probe. Beyond this radius the electron density decreases toward the walls. The plasma volume (negative glow) can be only estimated in an approximate way since the location of the sheath is not easy to determine. For the conditions depicted in the figure, the estimated radius of the plasma[51] is $\approx 2.5-3$ cm. At lower pressures, the curvature of the distribution is somewhat more pronounced. The mean electron temperature is approximately constant anywhere inside the glow.

The evolution of N_e and T_e with discharge pressure is displayed in the upper and middle panels of Figure 4. The electron densities represented here correspond to the densities averaged over the plasma volume. These are the values used for the model calculations. At 0.008 mbar, the lowest pressure investigated, the measured electron density is close to 1×10^{10} cm^{-3} and the corresponding electron temperature is 8 eV. With increasing gas pressure, N_e grows, whereas T_e decreases. At the highest pressure explored, 0.2 mbar, the electron density reaches a value of 3×10^{10} cm^{-3} and T_e drops to 2.5 eV. In the same figure the model T_e values giving the best fit to the measured ion concentrations are also shown. Note that they are always within the experimental uncertainty. The expected cathode current could be calculated in principle from the measured ion
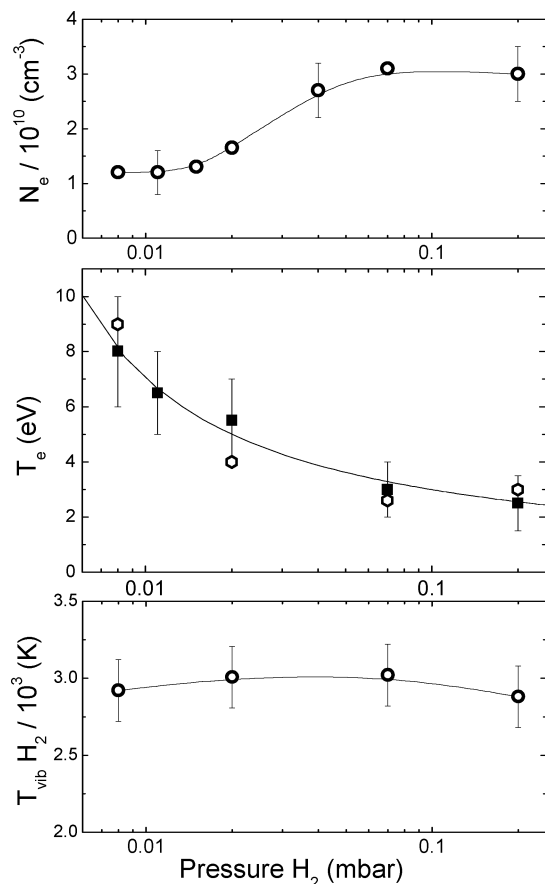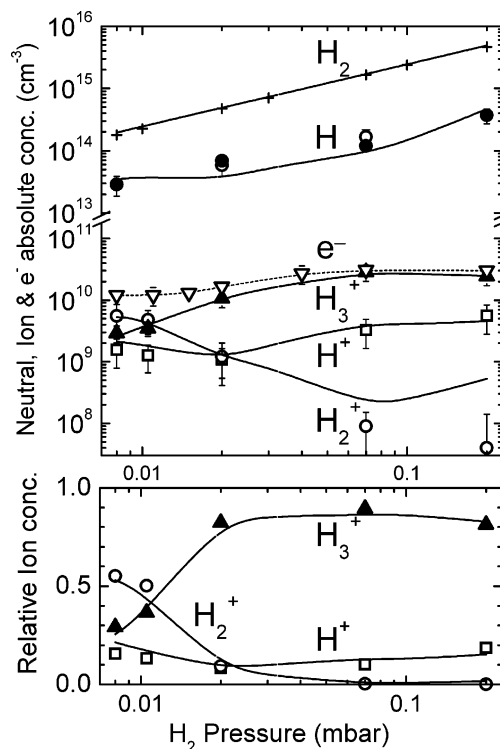
Figure 4. Upper panel: average electron densities as a function of pressure, for a 150 mA H_2 discharge, measured with the Langmuir probe. Middle panel: Electron temperatures. Black squares: Langmuir probe data with error bars. Open circles: values used in the model for best fit to the experimental concentrations of atoms and ions. Lower panel: H_2 vibrational temperatures obtained from optical emission spectroscopy (see text). The continuous lines are only to guide the eye.

Figure 5. Upper panel: Absolute concentrations of the various species in the H_2 plasma, as a function of pressure. Symbols: experimental data. Lines: model results. The closed circles in the H data correspond to the estimate based on the quotient between the $I_{H}\alpha$ and $I_{H}\beta$ emission lines; the open circles are from the actinometric measurements with Ar (see text). Lower panel: Relative concentrations of ions in the plasma. Symbols and lines are also the experimental data and model results, respectively.

concentration and temperature and using Bohm's velocity.[51] However, given the uncertainty in the actual plasma size and in the ion concentration at the "plasma edge" it is not easy to make a reliable prediction of the electrical current. Reasonable estimates may range from 100 to 350 mA, as compared with the actual value of 150 mA.

The lowest panel of Figure 4 shows the vibrational temperatures measured for the H_2 molecules in the plasma. In all cases they were found to be close to 3000 K. These temperatures are consistent with an effective electron impact excitation and a relatively inefficient relaxation of the vibrationally excited H_2 molecules, either at the walls or in gas-phase collisions. Recent work by Hassouni et al.[18] shows that H atoms, though present in a relatively small concentration, may be more efficient than H_2 molecules for the global quenching of the excited vibrational states. As indicated in the previous section, some of the rate coefficients for processes involving H_2 molecules and H_2^+ ions may be very sensitive to the vibrational temperature of the molecules and although the dynamics of vibrational excitation and deexcitation is not explicitly included in the kinetic model, the dependence of these rate coefficients on T_v is taken into account. The H_2 rotational temperatures determined from the emission measurements are in the 300−350 K range (not shown), and they correspond to the gas temperature within the experimental uncertainty.

The concentrations of the neutral and charged species in the plasma as a function of pressure are represented in the upper panel of Figure 5, together with the model simulations. The lower panel of this figure shows the relative concentrations of ions. As can be seen, the simulations are in good agreement with the measurements over the whole range of pressures investigated. Using the model calculations, we can now give a physical interpretation of the most relevant results.

Hydrogen atoms are produced basically in the electron impact dissociation of H_2 (reaction 13 of Table 1) and are lost in wall collisions, where they recombine to H_2 (reaction 1 of Table 2). Other sinks of atomic hydrogen play only a minor role. Overall, the fraction of atomic hydrogen is found to be between ∼17 and 7%. The largest relative concentration of H atoms (≈17%) appears at the lowest pressure, where the electron temperature is close to 8 eV and the dissociation of H_2 is more efficient. For higher pressures, the decrease of T_e causes a reduction in the dissociation rate coefficient, compensated only partly by the growth in electron density; as a consequence, the relative concentration of H atoms reduces to 8−10%. For the conditions of the present experiment, wall recombination, rather than diffusion, is found to be the rate-limiting step in the transformation of atomic hydrogen to H_2. There is a great disparity in the literature values for the recombination coefficients of H on stainless steel walls. For the simulation of the present experiments, a value of $\gamma = 0.03$ was used.[52] A much higher coefficient ($\gamma = 0.2$) was reported by Kae-Nune et al.,[53] but this value leads to much lower steady-state concentrations of H and is incompatible with the results of the present study. To test the contribution to H production of ions hitting the wall, the γ^+ values (Table 2) were changed in the model between 0 and 1; nevertheless the predicted [H] did not change significantly, even at the lowest pressures, where only a slight decrease

Low Pressure Hydrogen DC Plasmas

J. Phys. Chem. A, Vol. 110, No. 18, 2006 **6065**

in [H] for $\gamma^+ = 0$ was estimated. This [H] decrease was within the uncertainty of the experimental data. The same results were also found when ions were not included in the model. This agrees with our previous work on air plasmas,[34] where the irrelevance of ions in the kinetics of neutral species was confirmed.

In the weakly ionized plasma under consideration, the concentrations of ions are orders of magnitude lower than those of neutrals. The total ionization degree (N_e/N_{H_2}) changes by an order of magnitude over the range of pressures studied, but even at the smallest pressure studied, it is lower than 1×10^{-4}. The significant changes observed in the relative ion densities with increasing gas pressure, are worth noting (see lower panel of Figure 5). At the lowest pressures (below 0.01 mbar) the dominant ion is H_2^+, formed directly in the electron impact ionization of the hydrogen molecules (reaction 7 of Table 1), other processes leading also to H_2^+, like reactions 6 and 8, play a negligible role. At these low pressures, many of the formed ions can reach directly the wall without undergoing collisions. For higher pressures, the collision frequency increases and the H_2^+/H_3^+ ratio is determined by the $H_2 + H_2^+$ ion−molecule reaction (number 10 of Table 1). This barrierless process has a very large rate coefficient and transforms with great efficiency the primary H_2^+ ions into H_3^+ through collisions with the prevailing H_2 molecules. Through this mechanism, H_3^+ builds up to a relatively high concentration. As mentioned above, a ionic temperature equal to that of the neutrals has been assumed in the model simulations. This is a reasonable assumption for the present plasma, formed basically by a negative glow with a macroscopic electric field close to zero. Even if the temperature of the ions were higher than that of the neutrals, it is never expected to exceed 1 eV. For this energy range, the cross section[23] for the ion molecule reaction $H_2^+ + H_2 \rightarrow H_3^+ + H$ is $\sim(2-8) \times 10^{-14}$ cm^2. At $p = 8 \times 10^{-3}$ mbar, the corresponding mean free path is $\sim 0.5-2$ cm, comparable to the plasma radius. At this pressure, only 30% of the ions are in the form of H_3^+. Between 8×10^{-3} and 2×10^{-2} mbar, the concentration of H_3^+ grows proportionally to the increase in pressure (i.e., to the collision frequency) until it reaches a relative concentration of about 80%. The rates for reactions or charge-transfer processes of H_3^+ with other molecules or ions are thought to be very small at the temperatures considered in the present work and are ignored.[23] Collisions of H_3^+ with electrons have deserved much attention. In particular its electron impact neutralization (reactions 11 and 12 of Table 1) is the dominant mechanism of destruction of this ion in diffuse interstellar clouds, and although the results from different groups have converged gradually, the neutralization mechanisms and rate coefficients are still under debate (see, for instance comments in ref 54). As indicated above, the model uses the relatively large rate coefficients given in ref 31 and shown in Figure 2, which correspond to the most recent experimental cross sections.[49,54,55] An evaluation of these H_3^+ destruction mechanisms in our plasma shows them to be irrelevant as compared with wall collisions (reaction 3 of Table 2), which is by far the prevalent loss term. Because of the efficient transformation of H_2^+ into H_3^+ and to the lack of efficient gas-phase destruction processes, H_3^+ dominates the ion composition in the glow region over most of the pressure range studied. For pressures higher than 0.07 mbar, H_2^+ ions virtually disappear. In their work, Hollmann and Pigarov[31] found that, overall, the ion composition in the target region of their discharge is dominated by H_3^+ for $T_e < 5$ eV. This is also the electronic temperature range for which the H_3^+ ion is prevalent in the present plasma.

There is always a 10−20% fraction of H^+ ions which are formed mostly by collisions with electrons, either in the dissociative ionization of H_2 (reaction 2 of Table 1) or in the ionization of H atoms (reaction1 of Table 1) previously produced in the electron impact dissociation of hydrogen molecules. The two processes give comparable amounts of H^+ ions at the lowest pressure investigated, where the electron temperature is high ($T_e \approx 8$ eV). For higher pressures, i.e., lower electron temperatures, the contribution of reaction 2 becomes negligible. Overall, H^+ ions do not influence the concentrations of H_3^+ or H_2^+ and vice versa. As in the case of H_3^+ ions, H^+ has no efficient gas phase sinks and disappears essentially in collisions with the walls (reaction 2 of Table 2). The absolute concentration of H atoms grows by more than an order of magnitude over the pressure range studied, in contrast, that of H^+ ions only doubles; this is due to the marked drop (nearly 2 orders of magnitude) in the rate coefficient for direct ionization of H between 8 and 2.5 eV, which is only partly compensated for by the growth in electron density and by the increase of the ion lifetime, which varies from ~ 0.7 to 9.3 μs.

For some of the lowest pressure ($\sim 2 \times 10^{-3}$ mbar) target plasmas investigated by Hollmann and Pigarov,[31] the ion composition was dominated by the H^+ ions generated in the arc. In the present work, with different plasma production mechanism and much weaker ionization, this condition was never approached and H^+ constituted always a small fraction of the total ion density.

Summary and Conclusions

The kinetics of the hydrogen plasma formed in a 150 mA, hollow cathode dc discharge has been investigated over the 0.008−0.2 mbar range. The investigation is based on a detailed experimental diagnostics of the plasma, including the determination of electron densities and temperatures, the vibrational and rotational temperature of H_2, as well as the measurement of the concentration of the neutral and ionic species present.

A simple model of the plasma containing a reduced number of processes including electron impact, ion molecule reactions and heterogeneous recombination, can account satisfactorily for the experimental observations using literature rate constants.

The fraction of atomic hydrogen was found to vary between 0.17 and 0.07. A low recombination coefficient ($\gamma = 0.03$) of H atoms on the stainless steel walls of the reactor is needed in order to justify the observed concentration of H atoms and H^+ ions.

Between the lowest pressure and 0.02 mbar, significant variations in the ion composition are observed as the mean free path of the ions becomes smaller than the glow dimensions. The plasma changes from a condition where H_2^+ ions are dominant to another where mostly H_3^+ is observed, due to the efficient $H_2 + H_2^+ \rightarrow H_3^+ + H$ reaction. Beyond this pressure, the relative ion concentrations do not vary much. The H^+ ion is basically formed in the electron impact ionization of H_2 and H, and does not interconvert with the other two.

The present work shows that the relevant processes considered by Hollmann and Pigarov[31] to explain the characteristics of their reflex-arc discharge of H_2 can account for the properties of this different kind of plasma with comparable gas pressures, but appreciably lower electron density and much lower gas temperatures.

References and Notes

(1) Herbst, E.; Klemperer, W. *Astrophys. J.* **1973**, *185*, 505.

(2) Watson, W. D. *Astrophys. J.* **1973**, *183*, L17.

(3) Oka, T. *Phys. Rev. Lett.* **1980**, *45*, 531.

(4) McCall, B. J.; Oka, T. *Science* **2000**, *287*, 1941.

(5) Petrović, Z. L.; Jelenović, B. M.; Phelps, A. V. *Phys. Rev. Lett.* **1992**, *68*, 325.

(6) St-Onge, L.; Moisan, M. *Plasma Chem. Plasma Proc.* **1994**, *2*, 87.

(7) Gicquel, A.; Chenevier, M.; Hassouni, K.; Tserepi, A.; Dubus, M. *Appl. Phys.* **1998**, *83*, 7504.

(8) von Keudell, A.; Jacob, W. *Prog. Surf. Sci.* **2004**,.

(9) Gorse, C.; Capitelli, M.; Bacal, M.; Bretagne, J.; Lagana, A. *Chem. Phys.* **1987**, *117*, 177.

(10) Loureiro, J.; Ferreira, C. M. *J. Phys. D: Appl. Phys.* **1989**, *22*, 1680.

(11) Gorse, C.; Celiberto, R.; Cacciatore, R.; Lagana, M.; Capitelli, M. *Chem. Phys.* **1992**, *161*, 211.

(12) Garscadden, A.; Nagpal, R. *Plasma Sources Sci. Technol.* **1995**, *4*, 268.

(13) Matveyev, A. A.; Silakov, V. P. *Plasma Sources Sci. Technol.* **1995**, *4*, 268.

(14) Hassouni, K.; Gicquel, A.; Capitelli, M.; Loureiro, J. *Plasma Sources, Sci. Technol.* **1999**, *8*, 494.

(15) Capitelli, M.; Celiberto, R.; Gorse, C.; Laricchiuta, A.; Pagano, D.; Traversa, P. *Phys. Rev. E* **2004**, *69*, Art. No. 023504, Part 2.

(16) Laricchiuta, A.; Celiberto, R.; Janev, R. K. *Phys. Rev. A* **2004**, *69*, Art No. 022706.

(17) Shakhatov, V. A.; De Pascale, O.; Capitelli, M.; Hassouni, K.; Lombardi, G.; Gicquel, A. *Phys. Plasmas* **2005**, *12*, Art. No. 023504.

(18) Hassouni, K.; Lombardi, G.; Gicquel, A.; Capitelli, M.; Shakhatov, V. A.; De Pascale O. *Phys. Plasmas* **2005**, *12*, Art. No. 073301.

(19) Bacal, M.; Hamilton, G. W. *Phys. Rev. Lett.* **1979**, *42*, 1538.

(20) Kalache, B.; Novikova, T.; Fontcuberta i Morral, A.; Roca i Cabarrocas, P.; Morscheidt, W.; Hassouni, K. *J. Phys. D: Appl. Phys.* **2004**, *37*, 1765.

(21) Diomede, P.; Longo, S.; Capitelli, M. *Eur. Phys. J. D.* **2005**, *33*, 243.

(22) Tawara, H.; Itikawa, Y.; Nishimura, H.; Yoshino, M. *J. Phys. Chem. Ref. Data.* **1990**, *19*, 617.

(23) Phelps, A. V. *J. Phys. Chem. Ref. Data.* **1990**, *19*, 653.

(24) Celiberto, R.; Janev, R. K.; Laricchiuta. A.; Capitelli, M.; Wadhera, M.; Atems, D. E. *At Data Nucl. Data Tables* **2001**, *77*, 161.

(25) Celiberto, R.; Capitelli, M.; Laricchiuta, A. *Ohys. Scr.* **2002**, *T96*, 32.

(26) Capitelli, M.; Celiberto, R.; Esposito, F.; Laricchiuta, A.; Hassouni, K.; Longo, S. *Plasma Sources Sci. Technol.* **2002**, *11*, A7.

(27) Pigarov, A. Yu. *Phys. Scr.* **2002**, *T96*, 16.

(28) Albella, J. M.; Gomez-Aleixandre, C.; Sánchez-Garrido, O.; Vázquez, L.; Martínez-Duart, J. *Surf. Coat. Technol.* **1995**, *70*, 163.

(29) Lee, S. T.; Lin, Z.; Jiang, X. *Mater. Sci. Eng.* **1999**, *25*, 123.

(30) Marinkovic, S. N. *Chem. Phys. Carbon* **2004**, *29*, 71.

(31) Hollmann, E. M.; Pigarov, A. Yu. *Phys. Plasmas* **2002**, *9*, 4330. Numerical values for the rate coefficients used in this work were kindly provided by E. M. Hollmann to the authors.

(32) Hollmann, E. M.; Antar, G.; Doerner, R. P.; Luckhardt, S. C. *Rev. Sci. Instrum.* **2001**, *72*, 623.

(33) Geobel, D. M.; Campbell, G.; Conn, R. W. *J. Nucl. Mater.* **1984**, *121*, 27.

(34) Castillo, M.; Méndez, I.; Islyaikin, A. M.; Herrero, V. J.; Tanarro, I. *J. Phys. Chem. A* **2005**, *109*, 6225.

(35) Tabarés, F. L.; Tafalla, D.; Tanarro, I.; Herrero, V. J.; Islyaikin, A. M. *Vacuum* **2004**, *73*, 161.

(36) Tabarés, F. L.; Tafalla, D.; Tanarro, I.; Herrero, V. J.; Islyaikin, A.; Maffiotte, C. *Plasma Phys. Controlled Fusion* **2002**, *44*, L37.

(37) De los Arcos, T.; Domingo, Domingo, C.; Herrero, V. J.; Sanz, M. M.; Schultz, A.; Tanarro, I. *J. Phys. Chem. A* **1998**, *102*, 6282.

(38) Laframboise, J. G. Report No. 100. Institute of Aerospace Studies, University of Toronto: Toronto, Canada, 1966.

(39) Allen, J. E. *Plasma Sources Sci. Technol.* **1995**, *4*, 234.

(40) Schott, L. *Electrical Probes in Plasma Diagnostics,* Lochte-Holtgreven, W., Ed.: American Institute of Physics: New Yok 1995.

(41) *Eight Peak Index of Mass Spectra*; 4th ed.; Mass Spectrometry Data Centre, Royal Society of Chemistry: Cambridge, U.K., 1991.

(42) Lavrov, B. P.; Melnikov, A. S.; Käning, M.; Röpcke, J. *Phys. Rev. E* **1999**, *59*, 3526.

(43) Qing, Z.; Otorbaev, D. K.; Brussaard, G. J. H.; van de Sanden, M. C. M. *J. Appl. Phys.* **1996**, *80*, 1312.

(44) Lavrov, B. P.; Osiac, M.; Pipa, A. V.; Röpcke, J. *Plasma Sources Sci. Technol.* **2003**, *12*, 576.

(45) Lavrov, B. P.; Pipa, A. V. *At. Spectrosc.* **2002**, *92*, 709.

(46) Pipa A V, Ph.D. Thesis. On Determination of the Degree of Dissociation of Hydrogen in Non-Equilibrium Plasmas by Means of Emission Spectroscopy. Greifswald, Germany, 2004.

(47) Laborie, P.; Rocard, J. M.; Rees, J. A. *Tables de Sections Efficaces Électroniques et Coefficients Macroscopiques I Hydrogène et Gaz Rares*; Paris, Dunod: Paris, 1968.

(48) Anicich, V. G. *J. Phys. Chem. Ref. Data.* **1993**, *22*, 1469.

(49) Datz, S.; Sundström, G.; Biedermann, Ch.; Broström L.; Danared, H.; Mannervik, S.; Mowat, J. R.; Larsson, M. *Phys. Rev. Lett.* **1995**, *74*, 896.

(50) Chantry, P. J. *J. Appl. Phys.* **1987**, *62*, 220.

(51) Lieberman, M. A.; Lichtenberg, A. J. *Principles of Plasma Discharges and Materials Processing*; John Wiley & Sons: New York, 1994.

(52) Tserepi, A. D.; Miller, T. A. *J. Appl. Phys.* **1994**, *75*, 7231.

(53) Kae-Nune, P.; Perrin, Jerôme, Jolly, J, Guillon, J. *Surf. Sci. Lett.* **1996**, L495.

(54) Larson, M. *Annu. Rev. Phys. Chem.* **1997**, *48*, 151.

(55) Macko, P.; Ban, G.; Hlavenka, P.; Plasil, R.; Poterya, V.; Pysanenko, A.; Votava, O.; Johnsen, R.; Glosik, J. *Int. J. Mass. Spectrosc.* **2004**, *233*, 299.